

UC Riverside

UC Riverside Previously Published Works

Title

Fluorescamine Labeling for Assessment of Protein Conformational Change and Binding Affinity in Protein-Nanoparticle Interaction

Permalink

<https://escholarship.org/uc/item/3mc7w9w7>

Journal

Analytical Chemistry, 89(22)

ISSN

0003-2700

Authors

Duan, Yaokai
Liu, Yang
Shen, Wen
[et al.](#)

Publication Date

2017-11-21

DOI

10.1021/acs.analchem.7b02810

Peer reviewed



Published in final edited form as:

Anal Chem. 2017 November 21; 89(22): 12160–12167. doi:10.1021/acs.analchem.7b02810.

Fluorescamine Labeling for Assessment of Protein Conformational Change and Binding Affinity in Protein-Nanoparticle Interaction

Yaokai Duan, Yang Liu, Wen Shen, and Wenwan Zhong*

Department of Chemistry, University of California, Riverside, CA USA 92521

Abstract

Protein adsorption alters the “biological identity” of the nanoparticles (NPs) and could affect how biosystems respond to the invading NPs. Study of protein-NP interaction can help understand how the physicochemical properties of NPs impact the interaction and thus potentially guide the design of safer and more effective NPs for biomedical or other applications. Binding affinity between proteins and NPs, and the occurrence of protein conformational change upon binding to NPs are two important aspects to be learned, but few methods are currently available to assess both simultaneously in a simple way. Herein, we demonstrated that the fluorescamine labeling method developed in our group could not only reveal protein conformational change upon adsorption to NPs, owing to its capability to label the primary amines exposed on protein surface, but also it could be applied to measure the binding affinity. By screening the interaction between a large number of proteins and four types of NPs, the present study also revealed that protein adsorption onto NPs could be strongly affected by structure flexibility. The proteins with high structure flexibility experienced high degrees of conformation change when binding to the polystyrene NPs, which could potentially influence protein function. Overall, we demonstrate that our assay is a quick, simple, and high-throughput tool to reveal potential impacts on protein activity and evaluate the strength of protein-NP binding.

Once entering the physiological environment like blood and cell cytoplasm, engineered nanomaterials (ENMs) are known to adsorb proteins and form the “protein corona” which acts as the new “biological identity” of ENMs.^{1–7} The composition of protein corona can change dynamically, depending on interaction duration and the type and concentration of proteins in the environment.⁸ The more abundant proteins could be adsorbed first and then displaced by the low-abundance-but-high-affinity proteins after long duration, forming the

*Corresponding Author Wenwan.zhong@ucr.edu.

ASSOCIATED CONTENT

Supporting Information

The Supporting Information is available free of charge on the ACS Publications website. The content includes: Lists of the proteins and NPs used in this work with their properties; significance tests using MNOVA on the F/F_0 values displayed in Figure 1 and the PC1 and PC2 obtained from PCA shown in Figure 2a; loading factors of the PCA results shown in Figure 2b; LDA scores plot for MW, pI and GRAVY; impacts on the fluorescence of reacted fluorescamine from the PS NPs; protein properties plot; the original fluorescent signals from proteins during labeling; PCA score plots colored by MW, GRAVY and pI; B factors for four proteins; correlation between %adsorption of protein and F/F_0 ; fluorescence change ratios of HSA with PS48; impact of PS NPs on fluorescence; plots of fluorescence vs. particle concentration for three proteins; Hill plots of normalized fluorescence vs. particle concentration for different proteins; correlation between K_d and pI, MW and GRAVY.

stable “hard corona”.^{1,8–10} Different physiological outcomes could then occur to the ENMs depending on what proteins are adsorbed by the ENMs.^{1,4} For instance, serum albumin, found in the corona of silver, silica or polymer ENMs present in plasma could elongate their circulation time to facilitate uptake of the ENMs by the target cells, a property favored by ENMs employed as drug carriers, therapeutic reagents, or diagnostic tools.^{4,11–13} Transferrin adsorbed by the polystyrene and poly(glycidyl methacrylate) ENMs could actively target the breast or prostate cancer cells overexpressing transferrin receptor.^{8,14,15} However, serum albumin could reduce the targeting capability of such ENMs if co-existing in the surrounding environment,¹⁶ probably because albumin displaces transferrin off the ENM surface or interferes with receptor binding by covering up the binding sites on transferrin. Besides the type and affinity of the adsorbed proteins, changes to protein conformation upon adsorption could alter the biological responses to ENMs. Not only protein function could be impaired,¹⁷ but also the unfolded proteins could enhance uptake by immune cells, activate inflammation, as well as induce other side effects like blood coagulation, membrane structure damage and complement activation.¹⁸

The close correlation between protein adsorption and biological responses to ENMs calls for better understanding of the interactions between proteins and ENMs and how the interaction is affected by the properties of ENMs and proteins.^{2,10,13,19–21} The knowledge can guide the design of ENMs to promote the desired activity and suppress the potential adverse effects, improving the efficacy and safety of ENM implementation.²² Protein binding affinity and conformational change are two important aspects to be assessed in study of protein-ENM interaction. The most common tool for study of protein conformational change is circular dichroism (CD), which is widely available and simple to carry out. Hydrogen-deuterium exchange (HDX) or fast photochemical oxidation of proteins (FPOP) coupled with MS or NMR is more sensitive than CD and can provide details information about protein conformation.^{23,24} Moreover, chemical crosslinking coupled with MS has been used to explore protein conformational change as well as the binding sites of protein on ENMs.^{25,26} On the other hand, binding affinity can be measured using separation methods including ultracentrifugation,⁹ capillary electrophoresis (CE),²⁷ and size exclusive chromatography (SEC).¹⁰ Moreover, surface plasma resonance (SPR)¹⁰, quartz crystal microbalance (QCM)²⁸, isothermal titration calorimetry (ITC)¹⁰ and enzyme-linked immunosorbent assay (ELISA)²⁹ have been employed to study binding affinities and kinetics. However, the aforementioned techniques typically require expensive instruments, are time consuming and technically demanding, and could be compromised by the optical properties of ENMs. They are also not applicable for screening the interaction between a large number of proteins and ENMs. Fluorescence measurement provides high sensitivity and is compatible with high-throughput screening. Although it has been applied to measure the binding affinities of proteins on some ENMs taking advantage their intrinsic property in fluorescence quenching³⁰, it does not work for the ENMs not capable of generating changes in the optical properties of the interacting parties.

In our previous work, we have developed a fluorescence screening method that does not rely on the intrinsic optical properties of ENMs or proteins, but utilizes fluorescamine labeling to reveal protein-nanoparticle interaction in a rapid and high-throughput manner. We demonstrated that protein-nanoparticle binding could alter fluorescamine labeling of the

protein, and the resultant fluorescence patterns could differentiate the particles based on their core composition and size and surface properties.³¹ In the present study, we applied this assay to screen the interaction of a good number of proteins with two sets of nanoparticles, revealing the key protein properties that could influence protein-nanoparticle interaction and the close correlation between protein conformational change and fluorescamine labeling. We also showed that this method could be applied to evaluate the binding affinities. With the capability of assessing both protein conformational change and binding strength, our method should be very useful in revealing the key protein and ENM properties that govern protein-ENM interaction.

EXPERIMENTAL SECTION

Chemicals and Biochemicals.

Fluorescamine and all proteins were purchased from Sigma-Aldrich (St. Louis, MO). Dimethyl sulfoxide (DMSO), sodium phosphate monobasic monohydrate, anhydrous sodium phosphate dibasic, sodium chloride and bicinchoninic (BCA) assay kit were obtained from Fisher Scientific (Waltham, MA). Ultrapure water with electric resistance > 18.2M Ω was produced in-house, by the Milipore Milli-Q water purification system (Billerica, MA).

Nanoparticles.

The carboxylated polystyrene nanoparticles with an average diameter of 48 and 85 nm (PS48 and PS85) were obtained from Polysciences (Warrington, PA). The silica nanoparticles with an average diameter of 50 and 80 nm (Si50 and Si80) were purchased from nanoComposix (San Diego, CA).

Determination of protein properties.

Properties of protein, including molecular weight (MW), theoretical isoelectric point (pI), and the grand average of hydropathicity (GRAVY) value, were calculated based on protein sequences via the ProtParam tool available in ExPASy. All protein sequences were downloaded from NCBI. pI was calculated using pK values of amino acids described in Bjellqvist et al.³² The GRAVY value was calculated as the average of hydropathicity values of all amino acids in protein sequences.³³

Fluorescamine screening.

PS48 of 10 nM, PS85 of 3.2 nM, Si50 of 10 nM, or Si80 of 3.9 nM was incubated with 400 nM protein in the PBS buffer (10 mM phosphate at pH 7.4, 137 mM NaCl, and 2.7 mM KCl) for 1h at 37 °C. The different particle molarities provided similar surface areas for protein adsorption. Then, fluorescamine was added into the mixture at a final concentration of 1 mM, and incubated for 5 min, before fluorescence detection was carried out in the Victor II plate reader.

Data processing.

We defined F_0 as the fluorescence from the protein alone labeled by fluorescamine, and F as the fluorescence from the protein incubated with the NPs. Fluorescence change ratio (F/F_0) was calculated and subject to principal components analysis (PCA) using the R package 'ggfortify'.³⁴ The first two principal components were used for making the scores plots. In addition, k-means clustering was done by the same package. Significant test for fluorescence screening and PCA results were evaluated by MANOVA and linear discriminant analysis (LDA) with Jackknife prediction, with either the fluorescence change ratios or the first two principle values (PC1 and PC2) from PCA were used as the variables. For Jackknife prediction, all variables except one were used as the training set to classify proteins, and the one left out was used as the test set for test of assignment accuracy.

Measurement of NPs size.

PS48 NPs of 4 nM were incubated with different concentrations of HSA (0-12.8 μ M) in 1 \times PBS buffer for 1h at 37 °C, and were diluted 2,000 folds by 1 \times PBS. Nanoparticles Tracking Analysis (NTA) was used to measure the diameter of PS48 NPs after dilution, in which the Brownian motion of the NPs was monitored by a laser and converted to the hydrodynamic diameter.

Quantification of protein absorption and calculation of unit fluorescence.

The same concentrations of the NPs used in the aforementioned fluorescamine screening were incubated with 4 μ M protein for 1h at 37 °C. The incubation was split into four aliquots. Two were labeled by fluorescamine, and subject to fluorescence measurement. One of these two labeled samples was measured directly, while the other one was filtrated by a Vivaspin 500 centrifugal filter with a MWCO of 300kD (Sartorius AG, Goettingen, Germany) and the flow-through was collected for fluorescence measurement. The flow-through contained the free unbound protein and the NP-bound protein should stay on the membrane. The rest two aliquots were supplied with the same volume of the PBS buffer, and used for protein quantification by BCA. Similar to the fluorescamine labeled samples, one was measured without filtration and the other was filtrated and the flow-through was quantified. For both the fluorescamine labeled samples and the controls, the protein in the filtrate (the unbound protein) or the original solution (the total protein) were quantified by BCA assay after adjusting the volumes to be equal. Then the unit fluorescence was calculated by dividing the fluorescence signal by protein concentrations.

Measurement of binding affinity.

PS48 at various concentrations were incubated with 400 nM of the protein for 1h at 37 °C. Then, fluorescamine was added to label the protein, and fluorescence was measured by the Victor II plate reader. For each protein, the fluorescence intensity was normalized to 0-1, with the fluorescence of the control being 0 and the maximum fluorescence value as 1. Origin 8.0 was used to plot the curve and fit it with the Hills equation.

RESULTS AND DISCUSSION

Fluorescamine screening of protein-nanoparticle (NP) interaction.

Our previous work has demonstrated that fluorescamine labeling could detect protein-NP interaction.³¹ Fluorescamine is a fluorogenic dye that can rapidly react with the primary amines on proteins and become fluorescent. The fast reaction rate ensures that most of the labeling events occur to the solvent accessible primary amines on protein surface. Thus, protein-NP interaction could potentially change fluorescamine labeling by blocking the solvent accessible primary amines. Or, the interaction could induce protein unfolding to expose more amines, as proved by CD measurement in our previous work.³¹

If our labeling assay only relies on amine exposure from extensive protein unfolding, its applicability would be very limited. However, fluorescamine labeling is closely dependent on lysine reactivity, which is sensitive to solution pH as well as the microenvironment surrounding the lysine residues. While carrying out the labeling reaction in PBS buffer at pH 7.4 to match physiological conditions, we actually reduce the nucleophilicity of the amine groups on the lysine residues by protonation, yielding a reaction efficiency ~60%.^{35–37} But, when the lysine residue is in a hydrophobic environment or surrounded by amino acid residues with negative charges, its amine group would become less protonated and more reactive to fluorescamine. Since the surrounding of lysine residues could be altered when protein conformation varies, we expect our assay should be very sensitive to subtle protein conformational change induced by NP binding and is capable of evaluating NP binding to proteins with highly diverse properties.

To prove this, in the present study, we screened the interactions of the polystyrene particles (PS48 and PS 80) or the silica particles (Si50 and Si80) with a total of 21 proteins (Supporting Information, Table S1 & S2). The PS and silica Nps have been widely applied in drug delivery or biosensor designs,^{38–41} and thus understanding their behaviors in protein binding could help improve their effectiveness in biomedical applications. The selected proteins span a wide range of pI (isoelectric point), Mw (molecular weight) and hydrophobicity (represented by the GRAVY scores) (Figure S1, Supporting Information). We also included the compact, globular proteins and the intrinsically disordered proteins to see how protein tertiary structure could impact on NP interaction.⁴² Most of those proteins are abundant in biological fluids,⁴³ and thus expected to interact with ENMs entering biological systems.

Figure 1 shows the changes in fluorescamine labeling induced by incubation with the PS (Figure 1a) or silica NPs (Figure 1b). F_0 and F were the fluorescence resulted from fluorescamine labeling before (Figure S2, Supporting Information) and after particle incubation, respectively; and the ratio of F/F_0 from different proteins incubated with the PS or silica NPs were compared. When incubated with the PS NPs, most proteins exhibited F/F_0 larger than 1, indicating that more amines were labeled by fluorescamine upon binding to the NPs. In addition, PS48 typically induced larger fluorescence change than PS80, with most of the F/F_0 larger than 2. Larger variations in fluorescence change were observed when the proteins were incubated with the silica NPs. Most of the proteins experienced less than 50% change in fluorescence (i.e. $F/F_0 > 0.5$ or < 2). Multivariate analysis of variance

(MANOVA) also proved that the fluorescence changes induced by both PS48 and PS85 were significant, but those induced by Si50 and Si80 were not as significant as the PS NPs (Table S3, Supporting Information).

Dependence of protein-NP interaction on NP properties.

Protein-NP interactions are affected by electrostatic interaction, Van der Waals force, solvation, Brownian motion, etc.⁴⁴ Thus, differences in fluorescamine labeling could be caused by variations in NP properties. To reveal the correlation between the fluorescamine labeling profiles and NP properties, the statistical pattern recognition tool of PCA (Principal Component Analysis) was applied to visualize NP grouping based on the fluorescence change profiles of all 21 proteins shown in Figure 1. Each repetition of one protein-nanoparticle pair was viewed as one individual observation, and the proteins were treated as the variables. After PCA, 21 original variables were reduced to two principal components (PCs), PC1 and PC2, that summarized 67.6% and 17.2% of the total variance in the data set, respectively. The score plot of PC1 vs. PC2 (Figure 2a) indeed showed satisfactory grouping of the NPs: PC1 that represents the majority of the variance in our data separates the PS NPs from the silica particles based on core material difference; and PC2 separates the two PS NPs of different particle diameters. However, the two silica NPs of different diameters were not well separated (Figure 2a). The significant difference between the two PS particles and that between the PS and silica NPs were also confirmed by MANOVA on the two PC values, with the resultant p values for comparison between different NPs being < 0.001 except for that between the two silica NPs (Table S4).

The grouping effect illustrated by the PCA scores plot can be explained by differences in surface charge and core materials of the NPs. Zeta-potential measurement showed that the PS NPs carried much more negative charges on their surface than the Si NPs, which may cause stronger attachment of the cationic residues on the protein. Besides, the base material of PS NPs is composed of benzene rings that could interact more strongly with the hydrophobic regions on protein compared to the silica NPs covered by the hydrophilic silanol groups.⁴⁵ Moreover, the hydrophobicity of the PS core can decrease the pKa values of lysine residues getting close, which leads to less protonation on the amine groups and thus stronger nucleophilicity to react with fluorescamine.^{46,47}

The difference observed between the two PS particles could be mainly attributed to the variation in size. It has been reported that the sharper surface curvature on particles with a smaller diameter could induce more protein conformational change, which could lead to more primary amines to be labeled by fluorescamine.⁴⁸ Our previous work demonstrated the silica NPs with similar diameters but different surface charges could be differentiated. The outcomes from the represent and past studies support that, particle surface charge may play a more important role than their diameter in protein-NP interaction. The small fluorescence change in the silica NPs also subsidized any signal difference between the two silica NPs of different diameters.

Dependence of protein-NP interaction on protein properties.

Protein-NP interaction should be affected by protein properties as well. Compared to the standard NPs, proteins are more diverse in properties because they have large variations in amino acid sequences, secondary and tertiary structures, and surface properties, increasing the difficulty in sorting out the dominant protein characteristics that govern protein-NP interaction. To explore whether the fluorescamine labeling profiles resulted from protein-NP interaction could differentiate the proteins by their Mw, pI, or hydrophobicity, we carried out PCA but with the NPs being the variables. The two PC values obtained could summarize close to 70% of the overall variance of the data (Figure 2b), but no clear grouping of the proteins was observed. The loading factors analysis (Table S5, Supporting Information) showed that both the PS NPs had higher loadings in PC1, while the Si NPs were more decisive for PC2. Supervised clustering based on one protein property, i.e. Mw, pI, or GRAVY score (Figure S3, Supporting Information) did not show clear separation of the proteins, either. The poor grouping of proteins based on the properties listed in Table S1 was also verified by the poor prediction accuracies of Jackknife that only used Mw, pI, or GRAVY to build the LDA model (Table S6, Supporting Information), with < 60% of the proteins assigned accurately.

This is conceivable, because proteins are varied in many characteristic values, with no proteins only different by one or two properties while keeping the other(s) similar. In addition, the values of Mw, pI and GRAVY were calculated from the primary structures of the proteins, with no consideration of the secondary and tertiary structures nor the post translational modifications (PTMs). Since protein-NP interaction occurs between the surface of proteins and NPs, the surface properties are more important than the overall properties calculated from protein's amino acid sequence, which could be strongly affected by protein folding status and PTM and not be easily obtained.^{26,49}

We then applied the unsupervised clustering method, k-means clustering, on the PCA results with the NPs as the variables. This method can allow to classify the input dataset into k groups and visualize the relationship between samples in our dataset. Simply speaking, the distance between each data point and randomly selected centers was calculated, and the data points with the smallest square of the distance were viewed as similar data points and grouped together. Interestingly, the proteins were assigned into two groups, separated by PC 1 = 0 on the scores plot (Figure 2b). If examining the separation more closely, we found that the proteins grouped on the left panel of the PCA scores plot (PC1 < 0) are much more diverse in property, with no common structure features easily identified. On contrary, the group with PC1 > 0 included the proteins showing high fluorescence changes when incubated with NPs, the majority of which are with high structural flexibility. The most obvious one is beta- casein, an intrinsically disordered protein with the largest instability index among the proteins tested.⁴² It is less ordered in structure and more flexible than globular proteins like human serum albumin (HSA). Transferrin and conalbumin share high sequence similarity, and the crystal structures of both proteins show two lobes linked by flexible loops (Figure S4, Supporting Information).^{50,51} The relative position between the lobes is changing and unstable, as reflected by the high B factors found for the amino acids (a.a.) involved in the C terminal lobe of transferrin (Fig. S6): a higher B factor corresponds

to a higher mobility of the a.a. residue. Hemoglobin and catalase can form tetramers in solution, which are considered as a flexible structure as well.⁵²

The only exception is cytochrome c that contains high alpha helix contents and low B factors in its structure. However, it is worth noting that, ligand binding to cytochrome c could induce slight conformational change and cause disruption and rearrangement of the interactions such as hydrogen bonding and salt bridging between lysine residues.⁵³ Interestingly, hemoglobin and transferrin could have similar phenomena upon ligand binding. The well-known Bohr effect of hemoglobin describes that binding of oxygen could induce conformational change in hemoglobin and disrupt the salt bridges involving histamine and lysine residues, along with decrease of their pKa values and loss of protonation.⁵⁴ Upon binding or releasing of iron ions, the conformation of transferrin changes and is accompanied with deprotonation on lysine residues.⁵⁵ Therefore, we expect that when these proteins bind to NPs, similar effects could be induced and thus change the reactivity of the lysine residues towards fluorescamine, altering the labeling profile.

Protein adsorption on NPs and fluorescamine labeling.

With better understanding on how particle or protein properties could affect fluorescamine labeling, we went on to evaluate whether the fluorescence signal could reflect the amount of proteins adsorbed by the NPs. Such a correlation could allow affinity measure using our assay. We employed centrifugation to separate the free and NP-bound proteins. The centrifugal filter has a MWCO of 300 kDa that should pass the free proteins through but keep the large NPs with the adsorbed proteins on the filter top. We chose to evaluate the adsorption of 9 proteins on PS48, including transferrin, conalbumin, catalase, cytochrome C and hemoglobulin. These proteins showed higher fluorescence change than others when incubated with PS48. HSA was also tested to represent the proteins exhibiting medium-to-low fluorescence change.

The incubation procedure was carried out as done in the screening assay. The protein and NP mixture was added to the filter, and the free proteins eluted to the filtrate were quantified by BCA. The amount of proteins remained on the filter was then calculated and divided by the total amount of the protein used in the incubation to give out the %Adsorption plotted in Figure 3a. We can see from this plot that transferrin and conalbumin led to the highest %Adsorption, with close to 80% of the protein absorbed onto the PS48 NPs upon incubation. HSA yielded the lowest %Adsorption (< 50%), agreeing with its lower fluorescence changes than the other proteins during fluorescamine screening. Pearson correlation analysis showed that, except for the three proteins with high structure flexibility – transferrin, conalbumin, and catalase, the %Adsorption holds a strong linear correlation with the fluorescence change ratio F/F_0 (Figure S5, Supporting Information; Pearson correlation coefficient = 0.9756, p-value = 8.8E-4). This supports that, more proteins adsorbed, more amines would be labeled by fluorescamine. The three proteins with high structure flexibility also formed another linear relationship between F/F_0 and %Adsorption that had a smaller slope. They could experience a different degree of conformational change per unit mass of the adsorbed protein, than the other proteins.

The fluorescence signal detected from the protein and NP mixture is from both the free and the NP-bound proteins. To compare the degree of labeling in these two groups of proteins for better understanding of the relationship between adsorption and resultant fluorescence, we also filtered the incubation mixture that went through fluorescamine labeling. The fluorescence in both the mixture (before filtration) and the filtrate was measured and divided by the protein concentration in the corresponding solution, termed “unit fluorescence” (UF), which should reflect the degree of fluorescamine labeling per unit mass of the protein in the free or NP-bound proteins. The UF in the protein-PS48 mixture was much higher than that in the filtrate (Figure 3b), i.e. $UF_{mix}/UF_{free} \gg 1$, proving that the protein adsorbed on the NPs indeed experienced a higher degree of labeling compared to the free proteins, further proving that adsorption to the NPs changed protein conformation and activated more amine groups to be reactive with fluorescamine (Figure 3c).

Influence of protein or NP concentrations on the fluorescence profiles.

For our assay to properly reflect protein adsorption and conformational change, the molar ratio between the protein and NPs should be carefully chosen. If the protein amount is much higher than NPs, only a small portion of the protein could bind to the NPs, resulting in a small F/F_0 . Hence, influence of protein concentration on fluorescamine labeling was investigated. HSA was chosen as the model protein and the concentrations of HSA were changed from 40 nM to 8 μ M, with the NP concentration fixed at either 4 or 40 nM. After incubating HSA with PS48 for 1 hr at 37 °C, fluorescamine was added to the mixture for protein labeling. Agreeing with our assumption, the fluorescence change ratios (F/F_0) decreased with increasing protein concentration for both NP concentrations, indicating binding saturation at higher protein concentrations (Figure S6, Supporting Information).

A clearer relationship of fluorescamine labeling and adsorption saturation can be viewed by the normalized fluorescence change $(F-F_0)/(F_{max}-F_{min})$, with F_{max} and F_{min} being the highest or lowest fluorescence signals in the dataset, respectively (Figure 4a). The value of $(F-F_0)$ should represent the difference in the number of labeled amines before and after interaction with the NPs, and the normalization eliminates the random difference between data sets for clearer comparison. At lower protein concentrations between 40-200 nM, fluorescence increased gradually with protein concentrations (Figure 4a). This suggested that the surface areas of PS48 were enough to accommodate all HSA molecules, and with increasing protein concentrations, more proteins were adsorbed and experienced conformational change. When the concentrations of HSA increased further, such an increase slowed down, indicating that the proportion of HSA interacting with PS48 decreased, with fewer adsorption sites available. With the concentration of HSA higher than 2 μ M, the curve reached a plateau if the PS48 concentration was 4 nM (500:1 molar ratio of HSA:NPs, Fig. 4a). At this point, all active adsorption sites of PS48 were occupied by HSA and no more proteins could interact with PS48. To monitor the adsorption of HSA on PS48 NPs, size information of NPs was obtained via NTA under different protein/NPs ratios (Figure 4b). We can see the diameter of NPs increased with protein concentration and reached a plateau at $[HSA] = 2 \mu$ M. With a higher PS48 concentration of 40 nM, the fluorescence signal kept increasing, although with a lower slope. It was expected that a plateau would be reached with HSA concentration increasing beyond 20 μ M, but this concentration was outside of the

linear range of fluorescamine labeling for primary amines, and was not tested. The results indicate that the fluorescence signal should reflect the proportion of protein adsorbed and can possibly be used for evaluation of binding affinity if keeping the ratio of protein to NP below the saturation level.

NP could also influence fluorescence measurement. Similar to other organic fluorophores, the fluorescence of fluorescamine can be influenced by NPs, by either the inner filter effect (IFE) or the near-field effects including dynamic or static quenching, surface enhancement, and quantum yield variation, which depends on the position or distance of fluorescamine relative to the NPs.⁵⁶ In fact, these are the same concerns shared by using other optical methods to assess protein-NP interaction, especially when analyzing the luminescent NPs or those inducing strong light absorption or scattering.⁵⁷ To evaluate the impact from NPs to fluorescence measurement, we incubated 400 nM of the fluorescamine-labeled HSA with different concentrations of the PS NPs, and indeed observed some quenching of the fluorescence from the NPs: the fluorescence change ratio F/F_0 (with F being the fluorescence at the presence of NPs) increased linearly with particle concentration when $[NP] > 5$ nM (Figure S7 and S8 in Supporting Information). The bigger PS NPs showed larger influence, by increasing the fluorescence for ~ 50% at $[PS85] = 10$ nM; while < 20% change in fluorescence was observed for PS40 at 10 nM. Such an increase may be attributed to interparticle scattering.⁴⁹ In our screening, we kept the NP concentrations at 10 nM for PS48 or 3.2 nM for PS85, to keep the impact from NPs low (increasing the fluorescence by 1.1 or 1.2 folds) so that the measured fluorescence is only correlated to protein binding. Correction can also be applied for situations that large influence from NPs is observed taking advantage of the linear relationship between fluorescence change and NP concentration.

Assessment of the affinity of protein-NP interaction.

Fluorescamine labeling is sensitive to the reactivity of primary amines on the protein which could be strongly impacted by protein conformational change. Protein-NP interaction is likely to induce protein conformational change, making our assay valuable in interaction assessment. Our above results prove that if the appropriate protein and NP concentrations are used in our assay, the fluorescence change can be viewed as the signal of binding. Thus, the ratio can be plotted against NP concentration to obtain the binding curve of protein-NP interaction. We chose 13 proteins to explore their binding curves with PS48. These protein-particle pairs showed higher fluorescence changes than others. The fluorescence of avidin, aprotinin, and conalbumin increased with increasing PS48 concentration (from 0 – 6 nM) and reached a plateau at different $[PS48]$ (Figure S9, Supporting Information).

By plotting the fluorescence change at any NP concentration, i.e. $(F - F_0)$ after normalization with the maximum change at the plateau, i.e. $(F_{max} - F_0)$, verse NP concentration, we obtained the binding curves that can be fitted with the Hill equation (Figure 5 and Figure S9 for all 13 curves). The K_d (the macroscopic dissociation constant) was also calculated and listed in Table 3. In this fitting, the protein was viewed as the receptor, and the binding site on NPs were treated as the ligand, assuming that each NP were identical and carried the same number of binding sites. By monitoring the fluorescence

resulted from fluorescamine labeling of the protein upon binding to the NPs, we measured the change in the “receptor” when interacting with the ligand, matching well with the receptor-ligand binding model illustrated by the Hill equation.

From Table 1, we noticed that, the K_d values were not simply related to the size, pI, or hydrophobicity of the proteins, agreeing with the above PCA results (Table 1, Figure S11). Aprotinin has the smallest K_d among all proteins tested. It is a basic protein and carries positive charges to have electrostatic interaction with the negatively charged NPs. But the K_d values of two acidic proteins, antitrypsin and TCI, are also smaller than most of the other proteins. Conalbumin and transferrin are proteins with high homology, but different K_d values were obtained from our screening. It is worth noting that proteins with higher flexibilities, like beta-casein (an IDP protein), catalase, and transferrin, was proved to be weak binders with larger K_d values, although they showed large fluorescence change ratio in the screening at a fixed protein concentration (Figure 1). This indicates that a higher degree of conformational change in protein does not directly reflect stronger binding affinity. However, our assay is a convenient tool to assess both conformational change and binding affinity.

CONCLUSION

The present work demonstrated that fluorescamine labelling can be applied to evaluate binding between proteins with diverse properties and NPs, and the fluorescence should reflect protein conformational change caused by interaction with NPs. The impacts on the fluorescent signals from protein or particle concentrations were also evaluated to reveal the suitable protein and NP concentration ranges for affinity measurement using our assay. The study proves that, our method is convenient and rapid for assessment of protein-NP interaction, and fluorescamine labeling should reflect protein conformational change upon NP adsorption because of the high sensitivity of amine reactivity with the surrounding environment. Moreover, our assay can be used for evaluation of binding affinity using simple instrumentation. It is valuable to screen for proteins with higher binding affinities to NPs but experiencing lower conformational change which are useful for particle functionalization in biomedical research. On the other hand, conformational change may alter protein functions. For example, the metalloproteins screened in our study all underwent obvious conformational changes upon interacting with the negatively charged nanoparticles, indicating the potential adverse impact on protein functions by the charged PS nanoparticles. Follow-up studies on impact of NPs on the functions of such proteins are needed for toxicity evaluation.

Supplementary Material

Refer to Web version on PubMed Central for supplementary material.

ACKNOWLEDGMENT

Research reported in this publication was supported by the National Institute of Environmental Health Sciences of the National Institutes of Health under Award Number U01ES027293 as part of the Nanotechnology Health Implications Research (NHIR) Consortium. The content is solely the responsibility of the authors and does not necessarily represent the official views of the National Institutes of Health.

REFERENCES

- (1)Walkey CD, Chan WC. W. Chem. Soc. Rev. 2012; 41:2780–2799.
- (2)Lundqvist M, Stigler J, Elia G, Lynch I, Cedervall T, Dawson KA. Proc. Natl. Acad. Sci. U. S. A. 2008; 105:14265–14270. [PubMed: 18809927]
- (3)Monopoli MP, Walczyk D, Campbell A, Elia G, Lynch I, Bombelli FB, Dawson KA. J. Am. Chem. Soc. 2011; 133:2525–2534. [PubMed: 21288025]
- (4)Tenzer S, Docter D, Kuharev J, Musyanovych A, Fetz V, Hecht R, Schlenk F, Fischer D, Kiouptsi K, Reinhardt C, Landfester K, Schild H, Maskos M, Knauer SK, Stauber RH. Nat. Nanotechnol. 2013; 8:772–781. [PubMed: 24056901]
- (5)Albanese A, Walkey CD, Olsen JB, Guo H, Emili A, Chan WCW. ACS Nano. 2014; 8:5515–5526. [PubMed: 24797313]
- (6)Ahumada M, McLaughlin S, Pacioni NL, Alarcon EI. Anal. Bioanal. Chem. 2016; 408:1993–1996. [PubMed: 26847191]
- (7)Fang X, Duan Y, Liu Y, Adkins G, Zang W, Zhong W, Qiao L, Liu B. Anal. Chem. 2017
- (8)Milani S, Bombelli FB, Pitek AS, Dawson KA, Rädler J. ACS Nano. 2012; 6:2532–2541. [PubMed: 22356488]
- (9)Casals E, Pfaller T, Duschl A, Oostingh GJ, Puentes V. ACS Nano. 2010; 4:3623–3632. [PubMed: 20553005]
- (10)Cedervall T, Lynch I, Lindman S, Berggård T, Thulin E, Nilsson H, Dawson KA, Linse S. Proc. Natl. Acad. Sci. U. S. A. 2007; 104:2050–2055. [PubMed: 17267609]
- (11)Yan Y, Gause KT, Kamphuis MMJ, Ang C-S, O'Brien-Simpson NM, Lenzo JC, Reynolds EC, Nice EC, Caruso F. ACS Nano. 2013; 7:10960–10970. [PubMed: 24256422]
- (12)Lesniak A, Fenaroli F, Monopoli MP, Åberg C, Dawson KA, Salvati A. ACS Nano. 2012; 6:5845–5857. [PubMed: 22721453]
- (13)Gebauer JS, Malissek M, Simon S, Knauer SK, Maskos M, Stauber RH, Peukert W, Treuel L. Langmuir. 2012; 28:9673–9679. [PubMed: 22524519]
- (14)Singh R, Norret M, House MJ, Galabura Y, Bradshaw M, Ho D, Woodward RC, St Pierre TG, Luzinov I, Smith NM, Lim LY, Iyer KS. Small. 2016; 12:351–359. [PubMed: 26619362]
- (15)Kelly PM, Åberg C, Polo E, O'Connell A, Cookman J, Fallon J, Krpeti Ž, Dawson KA. Nat. Nanotechnol. 2015; 10:472–479. [PubMed: 25822932]
- (16)Salvati A, Pitek AS, Monopoli MP, Prapainop K, Bombelli FB, Hristov DR, Kelly PM, Åberg C, Mahon E, Dawson KA. Nat. Nanotechnol. 2013; 8:137–143. [PubMed: 23334168]
- (17)Wang J, Jensen UB, Jensen GV, Shipovskov S, Balakrishnan SV, Otzen D, Pedersen JS, Besenbacher F, Sutherland DS. Nano Lett. 2011; 11:4985–4991. [PubMed: 21981115]
- (18)Deng ZJ, Liang M, Monteiro M, Toth I, Minchin RF. Nat. Nanotechnol. 2011; 6:39–44. [PubMed: 21170037]
- (19)Röcker C, Pötzl M, Zhang F, Parak WJ, Nienhaus GU. Nat. Nanotechnol. 2009; 4:577–580. [PubMed: 19734930]
- (20)Wang H, Duan Y, Zhong W. ACS Appl. Mater. Interfaces. 2015; 7:26414–26420. [PubMed: 26571083]
- (21)Baptista P, Pereira E, Eaton P, Doria G, Miranda A, Gomes I, Quaresma P, Franco R. Anal. Bioanal. Chem. 2008; 391:943–950. [PubMed: 18157524]
- (22)Liu Y, Ren L, Yan D, Zhong W. Part. Part. Syst. Character. 2014; 31:1244–1251. [PubMed: 25580058]
- (23)Chen J, Rempel DL, Gau BC, Gross ML. J. Am. Chem. Soc. 2012; 134:18724–18731. [PubMed: 23075429]
- (24)Konermann L, Pan J, Liu Y-H. Chem. Soc. Rev. 2011; 40:1224–1234. [PubMed: 21173980]
- (25)Sinz A. Anal. Bioanal. Chem. 2017; 409:33–44. [PubMed: 27734140]
- (26)Zeng S, Huang YM, Chang CA, Zhong W. Analyst. 2014; 139:1364–1371. [PubMed: 24482794]
- (27)Li N, Zeng S, He L, Zhong W. Anal. Chem. 2010; 82:7460–7466. [PubMed: 20672831]

- (28)Hoshino Y, Koide H, Furuya K, Haberaecker WW, Lee S-H, Kodama T, Kanazawa H, Oku N, Shea KJ. *Proc. Natl. Acad. Sci. U. S. A.* 2012; 109:33–38. [PubMed: 22198772]
- (29)Yonamine Y, Hoshino Y, Shea KJ. *Biomacromolecules.* 2012; 13:2952–2957. [PubMed: 22813352]
- (30)Zhang X, Zhang J, Zhang F, Yu S. *Nanoscale.* 2017; 9:4787–4792. [PubMed: 28345718]
- (31)Ashby J, Duan Y, Ligans E, Tamsi M, Zhong W. *Anal. Chem.* 2015; 87:2213–2219. [PubMed: 25587850]
- (32)Bjellqvist B, Hughes GJ, Pasquali C, Paquet N, Ravier F, Sanchez JC, Frutiger S, Hochstrasser D. *Electrophoresis.* 1993; 14:1023–1031. [PubMed: 8125050]
- (33)Kyte J, Doolittle RF. *J. Mol. Biol.* 1982; 157:105–132. [PubMed: 7108955]
- (34)Tang Y, Horikoshi M, Li W. *The R Journal.* 2016; 8:478–489.
- (35)Castell JV, Cervera M, Marco R. *Anal. Biochem.* 1979; 99:379–391. [PubMed: 42326]
- (36)Muz M, Ost N, Kühne R, Schüürmann G, Brack W, Krauss M. *Chemosphere.* 2017; 166:300–310. [PubMed: 27705823]
- (37)De Bernardo S, Weigele M, Toome V, Manhart K, Leimgruber W, Böhlen P, Stein S, Udenfriend S. *Arch. Biochem. Biophys.* 1974; 163:390–399. [PubMed: 4859505]
- (38)Soppimath KS, Aminabhavi TM, Kulkarni AR, Rudzinski WE. *J. Control. Release.* 2001; 70:1–20. [PubMed: 11166403]
- (39)Baaske M, Vollmer F. *ChemPhysChem.* 2012; 13:427–436. [PubMed: 22213654]
- (40)Slowing II, Vivero-Escoto JL, Wu C-W, Lin VS-Y. *Adv. Drug Deliv. Rev.* 2008; 60:1278–1288. [PubMed: 18514969]
- (41)Slowing II, Trewyn BG, Giri S, Lin VSY. *Adv. Funct. Mater.* 2007; 17:1225–1236.
- (42)Redwan EM, Xue B, Almehdar HA, Uversky VN. *Curr. Protein Pept. Sci.* 2015; 16:228–242. [PubMed: 25714333]
- (43)Stempfer R, Kubicek M, Lang IM, Christa N, Gerner C. *Electrophoresis.* 2008; 29:4316–4323. [PubMed: 18956433]
- (44)Treuel L, Nienhaus GU. *Biophys. Rev.* 2012; 4:137–147. [PubMed: 28510093]
- (45)Miriani M, Eberini I, Iametti S, Ferranti P, Sensi C, Bonomi F. *Proteins: Struct. Funct. Bioinf.* 2014; 82:1272–1282.
- (46)Isom DG, Castañeda CA, Cannon BR, García-Moreno B. *Proc. Natl. Acad. Sci. U. S. A.* 2011; 108:5260–5265. [PubMed: 21389271]
- (47)Gleason NJ, Vostrikov VV, Greathouse DV, Koeppel RE. *Proc. Natl. Acad. Sci. U. S. A.* 2013; 110:1692–1695. [PubMed: 23319623]
- (48)Lundqvist M, Sethson I, Jonsson B-H. *Langmuir.* 2004; 20:10639–10647. [PubMed: 15544396]
- (49)Ashby J, Pan S, Zhong W. *ACS Appl. Mater. Interfaces.* 2014; 6:15412–15419. [PubMed: 25144382]
- (50)Kempner ES. *FEBS Lett.* 1993; 326:4–10. [PubMed: 8325386]
- (51)Duan Y, Jin H, Yu H, Wang Z, Zhang L, Huo J. *Mol. Simul.* 2013; 39:270–278.
- (52)Bourne Y, Grassi J, Bougis PE, Marchot P. *J. Biol. Chem.* 1999; 274:30370–30376. [PubMed: 10521413]
- (53)Capitanio G, Martino PL, Capitanio N, Papa S. *Biochim. Biophys. Acta, Bioenerg.* 2011; 1807:1287–1294.
- (54)Voet D, ; Voet JG. *Biochemistry* , 4th ed. ; Wiley : New York , 2011.
- (55)Baker HM, Baker EN. *Biometals.* 2004; 17:209–216. [PubMed: 15222467]
- (56)Zhang D, Nettles CB. *J. Phys. Chem. C.* 2015; 119:7941–7948.
- (57)Jain PK, Lee KS, El-Sayed IH, El-Sayed MA. *J. Phys. Chem. B.* 2006; 110:7238–7248. [PubMed: 16599493]

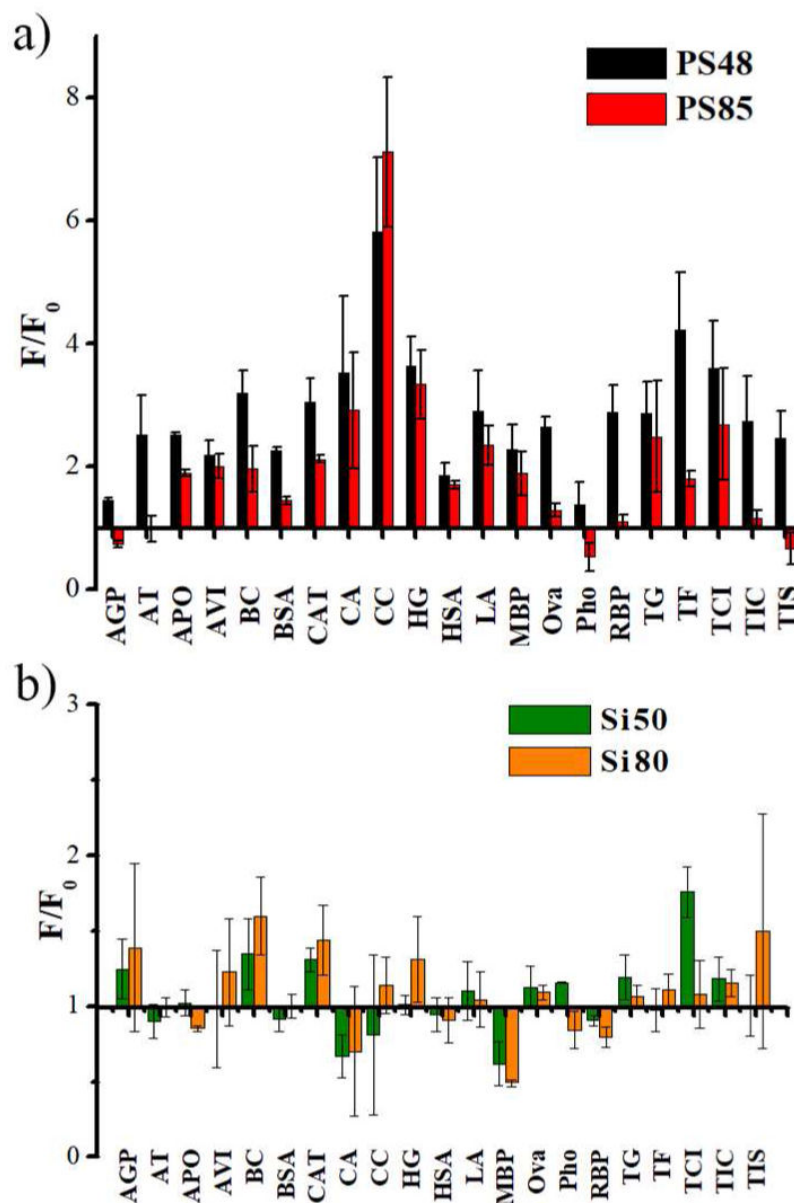


Figure 1. Fluorescamine labeling profiles of proteins with a) PS and b) Si nanoparticles. PS48 of 10 nM, PS85 of 3.2 nM, Si50 of 10 nM, or Si80 of 3.9 nM was incubated with 400 nM protein in the PBS buffer (10 mM phosphate at pH 7.4, 137 mM NaCl, and 2.7 mM KCl) for 1h at 37 °C. Then fluorescamine was added to final concentration of 1mM, and incubated for 5min before fluorescence signals being measured. Fluorescence signals change ratio (F/F₀) were calculated by dividing the signal of protein-NP pairs (F) by that of controls (F₀).

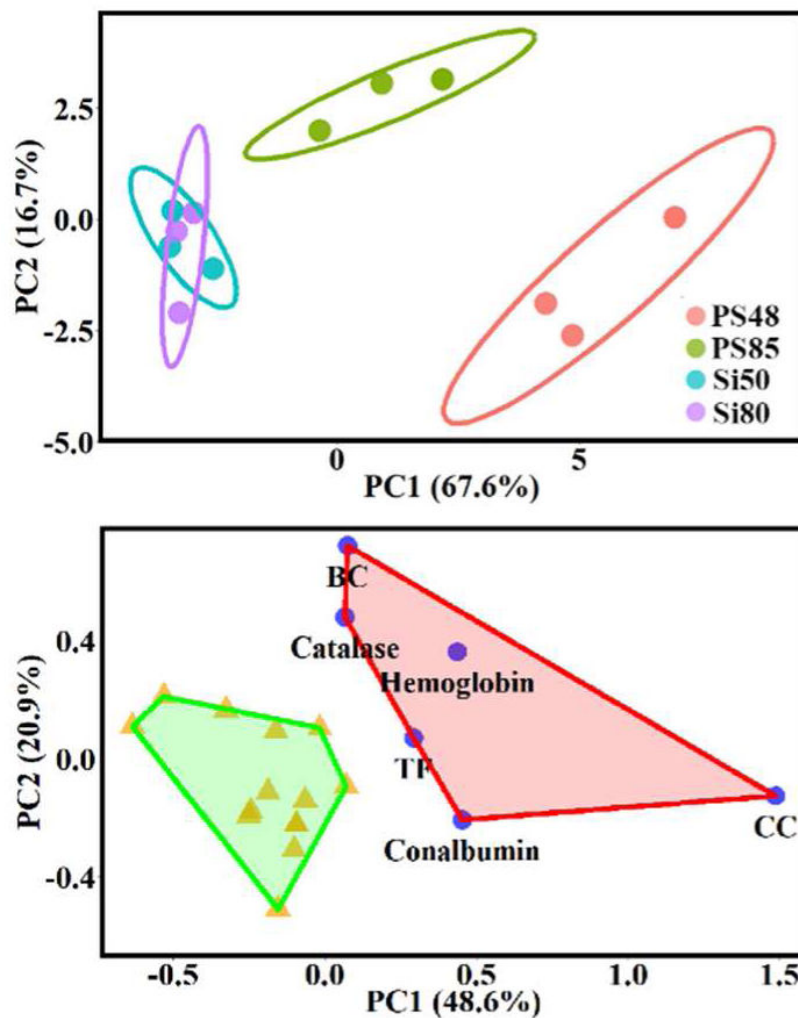


Figure 2. PCA scores plots obtained by a) treating the proteins as the variables to group the NPs; and b) treating the NPs as the variables to group the proteins and assigning the proteins by the boundaries determined by k-means clustering. Three repeats were evaluated. Ellipses shown were at 95% confidence.

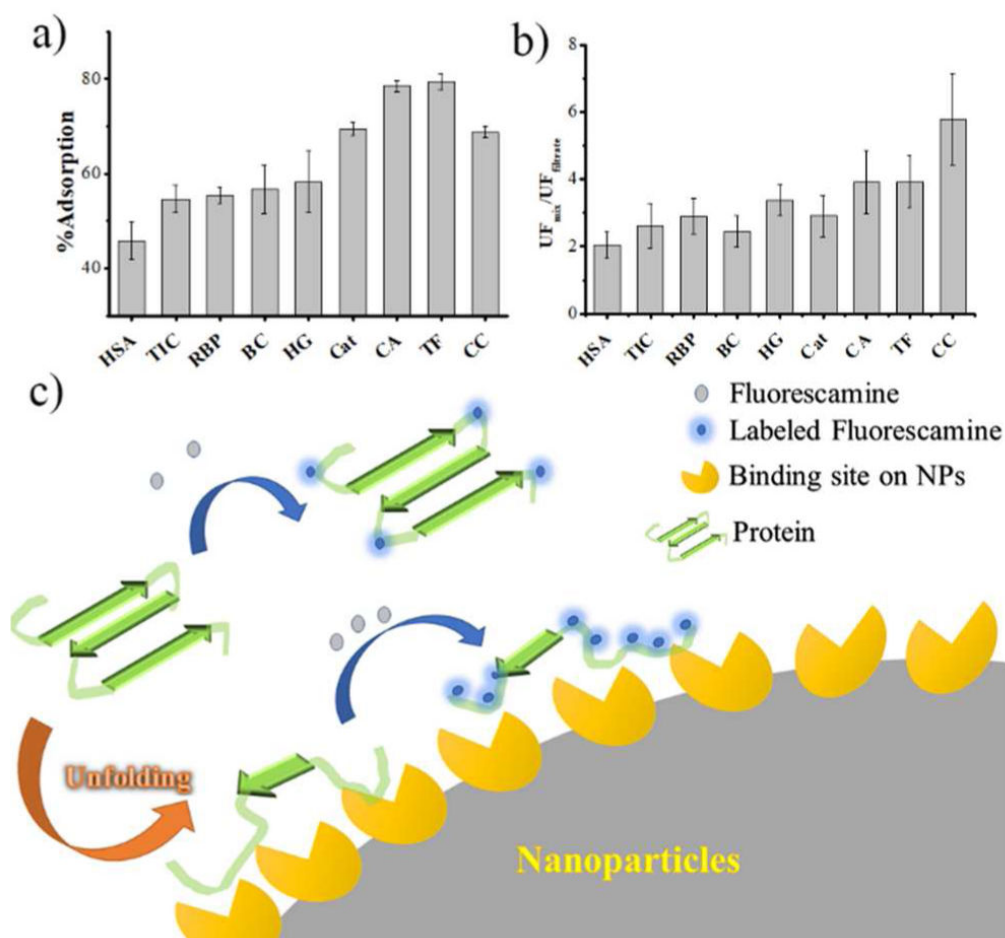


Figure 3. Comparison of a) % Adsorption of each protein on PS48, and b) ratio of unit fluorescence of each protein in the incubation mixture and in the filtrate. c) Illustration of fluorescence signal increase upon protein binding to the NPs. The bound protein would undergo conformational change that increases lysine reactivity with fluorescamine, and results in increased fluorescence signal.

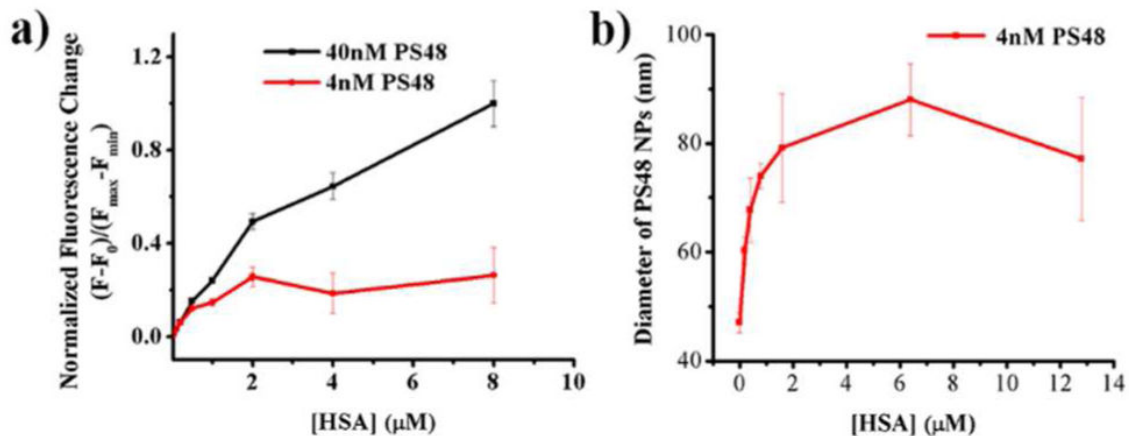


Figure 4.

a) Normalized fluorescence change of HSA incubated with PS48 at 40 or 4 nM.

Fluorescamine was added at a final concentration of 1mM. The change between fluorescence of HSA incubated with PS48 NPs (F) and that of HSA itself (F_0) was normalized to 0-1 using F_{\max} and F_{\min} in the dataset for better visualization. b)

Hydrodynamic diameter of PS48 NPs changed along with HSA concentrations. Sizes were measured by NanosightTM (Malvern Instruments) using the Nanaoparticle Tracking Analysis software, after PS48 NPs were incubated with different concentrations of HSA (0-12.8 μM) in PBS buffer for 1 hr at 37 μC .

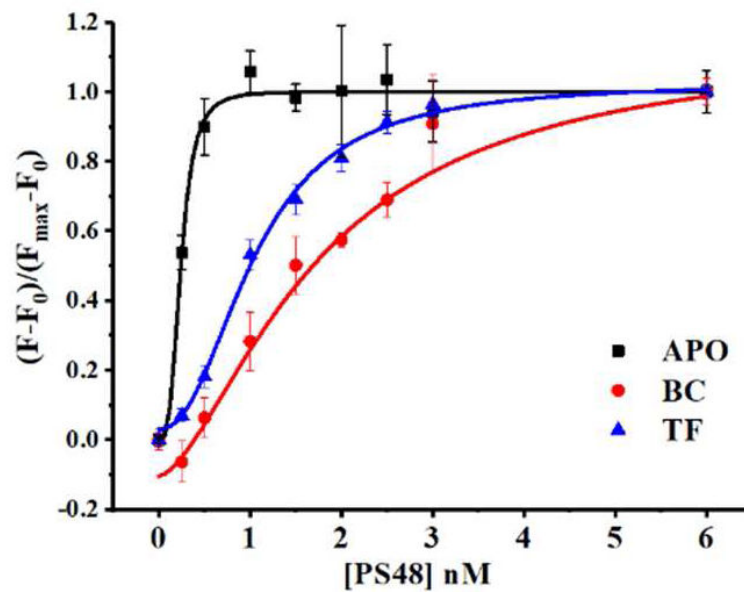


Figure 5. Normalized fluorescence of aprotinin, beta casein, and transferrin, under different PS48 concentrations. All proteins were at 400nM. Fluorescamine was added to a final concentration of 1 mM after proteins were incubated with PS48 in PBS for 1 hr at 37°C. For each protein, fluorescence signals were normalized to that with highest PS48 concentrations. Hills fitting was conducted with Origin 8.0 (OriginLab Corp.).

Table 1.

Dissociation constants (K_d) calculated from the binding curves. All proteins were in 400nM.

Protein	$K_d(\mu\text{M})$	Protein	$K_d(\mu\text{M})$
APO	0.24±0.16	HG	0.81±0.24
AT	0.45±0.23	LA	0.61±0.06
AVI	1.07±0.25	MBP	0.96±0.12
BC	1.75±0.33	OVA	1.03±0.07
BSA	1.43±0.56	RBP	1.57±0.24
CA	0.63±0.08	TCI	0.39±0.23
Cat	0.91±0.05	TF	1.05±0.07
CC	0.95±0.07	TIC	0.56±0.09
HSA	1.29±0.07		